ISSN No: -2456-2165 https://doi.org/10.38124/ijisrt/26apr929

Design of a Wind Turbine Blade Airfoil Profiles Suitable for Operation in Low Wind Speed Environment

Aliyu Abubakar[1]; Mutari Hajara Ali[2]

[1]Department of Electrical and Electronics Engineering, Federal Polytechnic, Bali. Taraba State.
[2]Department of Physics, College of Natural and pharmaceutical sciences, Faculty of Physical Sciences, Bayero University, Kano, Nigeria.

Publication Date: 2026/05/11

Abstract: This work presents the design of a wind turbine blade airfoil profile tailored for efficient operation in low-wind-speed environments. Baseline geometries were selected from low-Reynolds-number airfoils (NACA 2412, NACA 4412, NACA 4418, and NACA 4421). Optimization was carried out using the Non-dominated Sorting Genetic Algorithm II (NSGA-II), which systematically adjusted key geometric parameters camber, thickness distribution, leading-edge radius, and trailing-edge angle to enhance aerodynamic efficiency. Candidate airfoils were evaluated in terms of lift coefficient, cross-sectional area, and pressure coefficient distribution, subject to aerodynamic and structural constraints. The optimization process produced a Pareto front of feasible solutions, from which the optimal profile was selected. Results demonstrate that the optimized airfoils provide improved lift-to-drag performance and reduced cut-in wind speeds compared to baseline designs. These findings confirm that targeted aerodynamic optimization can significantly increase energy capture in low-wind-speed regions, thereby broadening the applicability of wind turbines in areas with limited wind resources.

Keywords: *Airfoil Optimization, NSGA-II, Lift-to-Drag Ratio, Low Wind Speed, Wind Turbine.*

How to Cite: Aliyu Abubakar; Mutari Hajara Ali (2026) Design of a Wind Turbine Blade Airfoil Profiles Suitable for Operation in Low Wind Speed Environment. *International Journal of Innovative Science and Research Technology*, 11(4), 4050-4059. https://doi.org/10.38124/ijisrt/26apr929

I. INTRODUCTION

Wind energy has emerged as one of the most rapidly expanding renewable energy sources, playing a crucial role in sustainable power generation and energy diversification(Sayed et al., 2012). The fundamental principle behind wind technology is the conversion of the wind's kinetic energy into mechanical energy through rotor blades, which is subsequently transformed into electrical energy by a generator. Importantly, the aerodynamic efficiency of horizontal-axis wind turbine blades governs their ability to capture energy, initiate rotation, and maintain stable operation(Liang et al., 2021). However, in regions where wind availability is low, this efficiency faces significant limitations.

In low-wind-speed regions such as inland areas of West Africa (e.g., Northern Nigeria, Niger) and parts of Southeast Asia, blade aerodynamics become particularly critical(Najar & Harmain, 2018). A major barrier to efficient operation is the cut-in speed the minimum wind velocity required to initiate energy production. In many of these resource-scarce regions, average wind speeds often remain below this threshold, leading to consistently poor energy yields(Robles-ocampo & Lastres, 2020). To overcome this challenge, specialized blade designs are necessary, particularly those optimized for low Reynolds number conditions.

Addressing the issue of low wind availability requires designing airfoils that can achieve high lift at low Reynolds numbers (Re) while maintaining stall resistance and structural robustness(Nouh, 2025). Such designs must balance aerodynamic performance with material durability, ensuring that turbines can both capture sufficient energy and withstand environmental stresses(Zhang et al., 2018). Previous studies have attempted to resolve this challenge, but their scope and methodologies reveal critical gaps(Amer et al., 2024).

Several prior studies have sought to optimize airfoil geometry for low-wind applications, ranging from parametric modifications of camber and thickness to computational methods such as single-objective genetic algorithms(Basu et al., 2016). While these approaches yielded encouraging improvements, many relied on

ISSN No: -2456-2165 https://doi.org/10.38124/ijisrt/26apr929

oversimplified aerodynamic models or limited optimization scopes(Zhao et al., 2020). As a result, unresolved trade-offs persist among lift, drag, and structural constraints, making them insufficient for robust, real-world application(Hussain et al., 2021). In light of these limitations, this research introduces a more comprehensive and effective optimization strategy.

This study proposes a multi-objective optimization framework specifically tailored for low-wind-speed turbine operation. By integrating NSGA-II with detailed aerodynamic analysis, the framework systematically refines baseline NACA airfoils to maximize lift-to-drag ratio, minimize cut-in speed, and ensure structural feasibility. The novelty of this work lies in its combination of evolutionary optimization with a rigorous aerodynamic objective formulation, providing a more practical solution to the challenges of low-wind-speed performance.

II. FUNDAMENTAL EQUATIONS AND OBJECTIVE FUNCTION FORMULATION

The aerodynamic performance of wind turbine blades in low wind speed conditions was investigated using NACA 2412, 4412, 4418, and 4421 profiles(Najar & Harmain, 2018). The flow behavior is characterized by the Reynolds number (Re), which is fundamental to analyzing fluid flow over the airfoil(Subashchandran, 2021). The governing equations for surface profiles, pressure coefficients, lift, and area define the optimization objectives. NSGA-II is then employed to balance maximizing lift and minimizing cross-sectional area, guiding airfoil designs toward Pareto-optimal solutions for improved low-speed turbine performance(Sayed et al., 2012).The Reynolds number is defined as:(Knap & Graczykowski, 2025)

$$R_e = \frac{Vc}{\mu} \tag{1}$$

Where: Re is the Reynolds number (dimensionless), rho is the air density (kg/m^3), V is the free-stream velocity (m/s), c is the chord length of the airfoil (m), and mu is the dynamic viscosity of air (Pa).

➢ *Objective Function Formulation*

The objective function formulation provides the foundation for applying multi-objective optimization techniques to this aerodynamic problem(Basu et al., 2016). It defines the performance goals of maximizing lift and minimizing cross-sectional area, which are crucial for achieving efficient airfoil designs at low wind speeds(Liu et al., 2020). This framework ensures a balance between aerodynamic efficiency and structural practicality.

- *Objective 1: Maximize Lift Coefficient (C_L)*

The goal is to enhance the airfoil's ability to generate lift under given operating conditions. Since lift is the primary force enabling energy capture, maximizing C_L directly improves performance at low wind speeds (Thiele et al., 2023).

✓ *Governing Equation:*

The lift coefficient is calculated from the pressure distribution around the airfoil:(Amer et al., 2024)

$$C_L(x) = \frac{1}{c}\oint (C_{pl} - C_{pu})dx \tag{2}$$

Where C_L is the lift coefficient, c is the chord length, C_{PL} is the pressure coefficient on the lower surface, C_{Pu} is the pressure coefficient on the upper surface, and dx is the differential length along the chord.

✓ *Design Formulation:*

This objective is formulated as a maximization problem:(Hussain et al., 2021)

$$Maximize(x) = C_L(x) = \frac{1}{c}\oint (C_{Pl} - C_{pu})dx \tag{3}$$

- *Objective 2: Minimize Cross-Sectional Area (A)*

Minimizing the cross-sectional area helps reduce material usage and aerodynamic drag, ensuring the design does not result in bulky or inefficient shapes(Ismaiel, 2023).

✓ *Governing Equation:*

The area is defined as the integral of the difference between the upper and lower surface coordinates:(Sumair et al., 2021)

$$A(x) = \int_0^c (y_u(x) - y_L(x))\,dx \tag{4}$$

Where A is the cross-sectional area, $y_u(x)$ is the y-coordinate of the upper surface, and $y_L(x)$ is the y-coordinate of the lower surface.

✓ *Design Formulation:*

This objective is formulated as a minimization problem:(Machado & Dutkiewicz, 2024)

$$Minimize f_2(x) = A(x) = \int_0^c (y_u(x) - y_L(x))\,dx \tag{5}$$

➢ *Airfoil Geometry and Pressure Distribution*

The geometry of a NACA 4-digit series airfoil is defined by its camber and thickness distribution. The upper and surface profiles are derived from the camber line $y_c(x$ and the standard NACA thickness distribution $y_L(x$)[9].The NACA thickness distribution is given by(Sayed et al., 2012):.

ISSN No: -2456-2165 https://doi.org/10.38124/ijisrt/26apr929

- *Upper Surface Profile:*

$$y_u(x) = y_c(x) + \frac{t}{0.2}c\left[0.2969\sqrt{\frac{x}{c}} - 0.1260\frac{x}{c} - 0.3516\left(\frac{x}{c}\right)^2 + 0.2843\left(\frac{x}{c}\right)^3 - 0.1015\left(\frac{x}{c}\right)^4\right] \quad (6)$$

And

- *Lower Surface Profile:*

$$y_L(x) = y_c(x) - \frac{t}{0.2}c\left[0.2969\sqrt{\frac{x}{c}} - 0.1260\frac{x}{c} - 0.3516\left(\frac{x}{c}\right)^2 + 0.2843\left(\frac{x}{c}\right)^3 - 0.1015\left(\frac{x}{c}\right)\right. \quad (7)$$

The pressure distribution, which is critical for calculating lift, is defined by the pressure coefficient C_p on the upper and lower surfaces (Liang et al., 2021):

$$C_{Pu}(x) = 1 - \left(\frac{V_u(x)}{V\infty}\right)^2 \quad (8)$$

And

$$C_{pl}(x) = 1 - \left(\frac{V_l(x)}{V\infty}\right)^2 \quad (9)$$

Where $V_L(x)$ and $V_L(x)$ are the local flow velocities on the upper and lower surfaces, respectively, and $V\infty$ is the free-stream velocity.

III. MATERIALS AND METHODS

The design of an efficient blade is affected by several factors, including aerodynamic performance (lift, drag, moment coefficients), structural integrity (stress, stiffness, cross-sectional area), material properties, and manufacturability. This study primarily focuses on the aerodynamic factors of lift and cross-sectional area (as a proxy for structural volume and drag).This study utilized NACA 2412, 4412, 4418, and 4421 as baseline profiles. Aerodynamic evaluations were performed through computational fluid dynamics (CFD) simulations integrated with MATLAB R2023b. The XFOIL engine was integrated within the optimization loop for rapid and accurate analysis of viscous flow at low Reynolds numbers (Re ≈ 200,000 - 500,000). The Non-dominated Sorting Genetic Algorithm II (NSGA-II) was used to maximize lift coefficients while minimizing cross-sectional areas under specific constraints (e.g., maximum thickness, leading-edge radius) [8].The optimization began with an initial population of baseline airfoils. The algorithm iteratively modified geometric parameters (camber, thickness, leading-edge radius) and evaluated performance metrics. Feasible solutions were kept on the Pareto front, while infeasible designs were penalized. Genetic operator's tournament selection, simulated binary crossover, and polynomial mutation were applied for 200 generations until convergence criteria were met. The optimal airfoil was selected from the non-dominated solutions based on the highest lift-to-drag ratio.

ISSN No: -2456-2165 https://doi.org/10.38124/ijisrt/26apr929

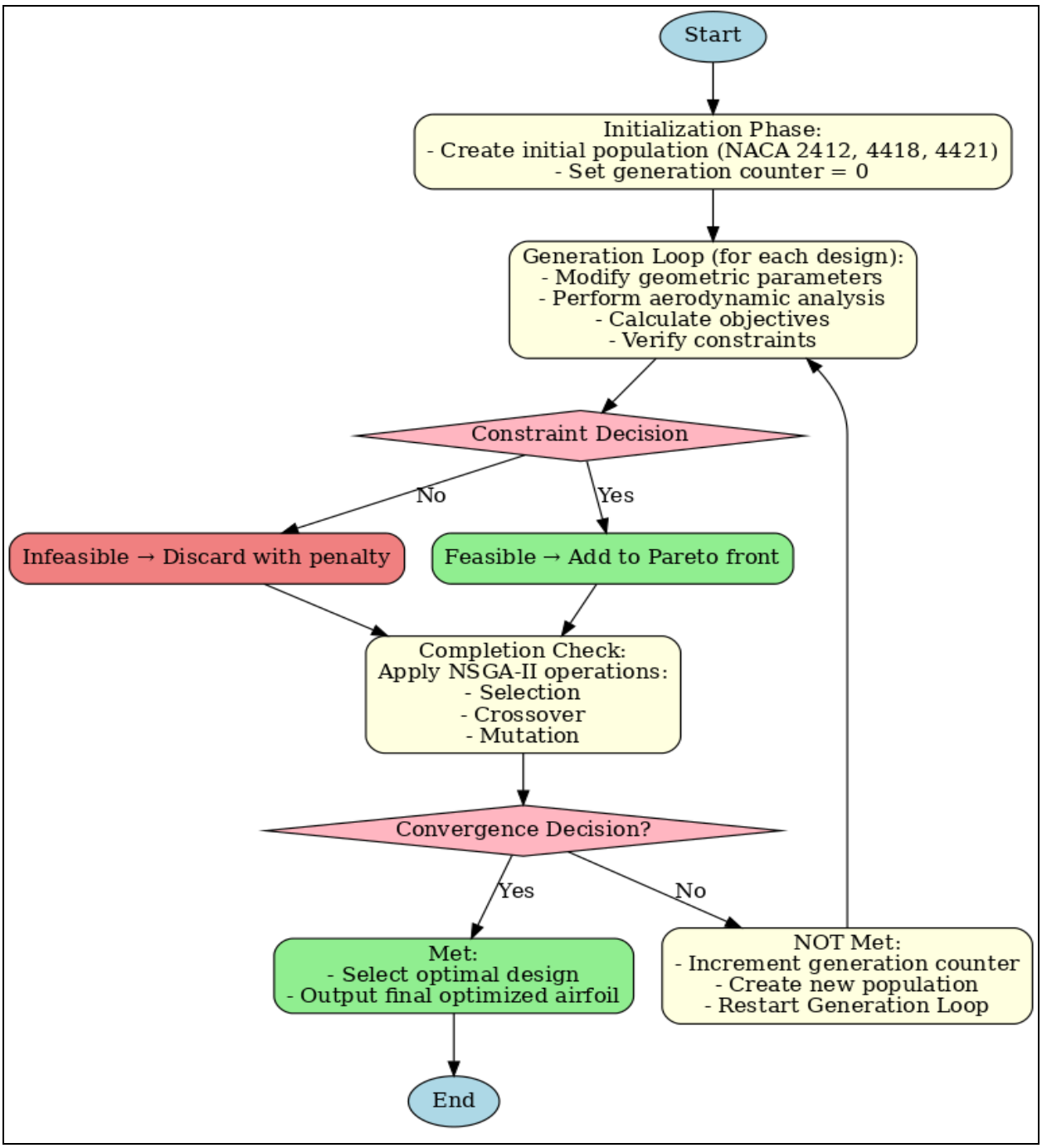

Fig 1 Standardized Flowchart of the NSGA-II Optimization Process Used in the Study.

Furthermore, a diagram of a representative optimized wind turbine blade, highlighting the airfoil profile at different spanwise locations (root, mid-span, tip) with key dimensions like chord length (c) and twist angle, is provided in Figure 2.

Figure 2 Schematic of a wind turbine blade showing optimized airfoil profiles at different spanwise sections (root, mid, tip) with chord length (c) and twist angle annotations.

ISSN No: -2456-2165 https://doi.org/10.38124/ijisrt/26apr929

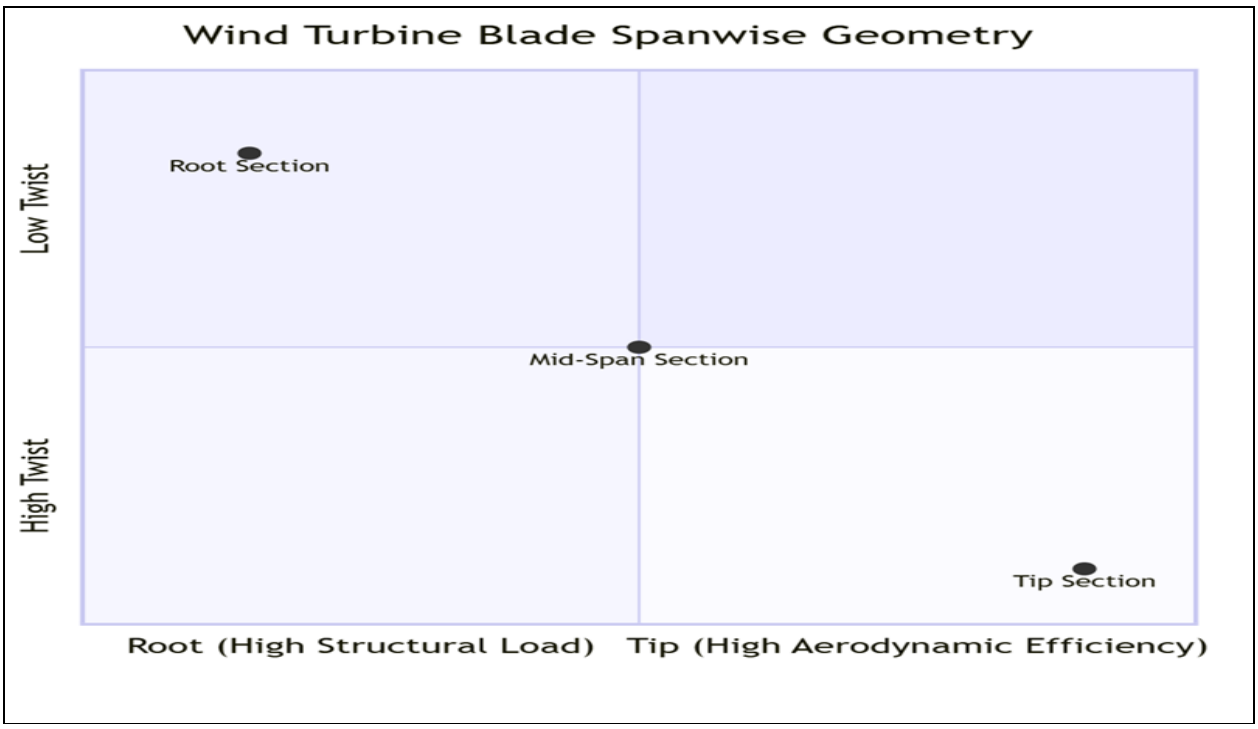

Fig 2 Schematic of a Wind Turbine Blade Showing Optimized Airfoil Profiles

IV. RESULTS AND DISCUSSION

This section presents the optimization results for the four airfoil profiles. For each airfoil, the optimized profile shapes are illustrated alongside their performance metrics. The analysis focuses on the lift coefficient ($\mathbb{C}_{\mathbb{L}}$) and the cross-sectional area (A), which are critical for evaluating aerodynamic performance and structural efficiency, respectively.

➢ *NACA 2412 Optimization*

Table 1 Results of the Optimization of NACA 2412.

	Airfoil	Original Lift Coefficient	Lift Coefficient of Optimized Airfoils	Area Reduction (%)
1	NACA 2412	1.6432	(a) 1.7498	5.2200
2			(b) 1.7427	2.1300
3			(c) 1.7494	3.5700

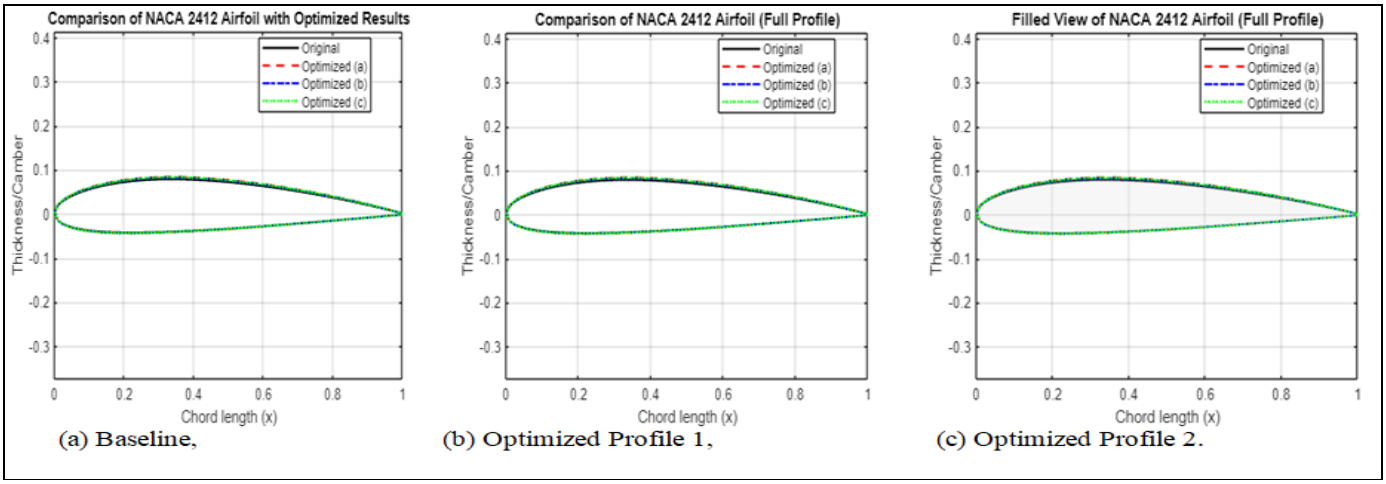

Fig 3 Optimized Airfoil Profile Shapes for NACA 2412:

ISSN No: -2456-2165 https://doi.org/10.38124/ijisrt/26apr929

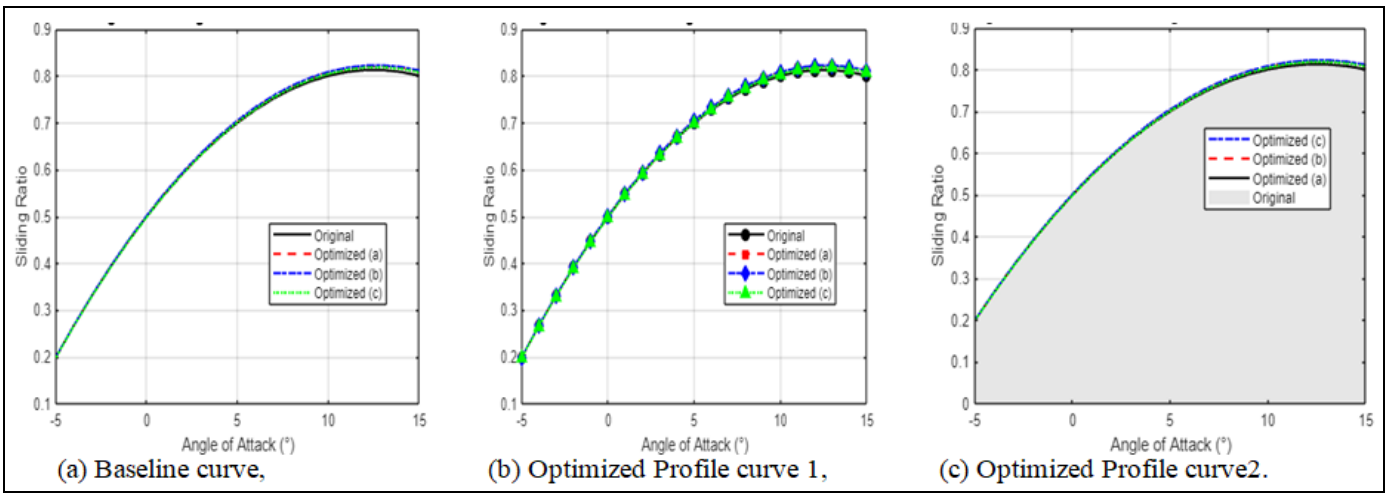

Fig 4 Design Results Showing Lift-to-Drag Polar for Baseline and Optimized NACA 2412 Airfoils.

Table 1 presents the design parameters and results for the NACA 2412 airfoil optimization. The data reveals an improved lift-to-drag performance, with the optimized profile achieving higher aerodynamic efficiency across a broader range of angles of attack compared to the baseline. This enhancement makes the optimized NACA 2412 suitable for energy extraction under very low wind speed conditions, where maximizing efficiency is critical for overcoming the cut-in speed barrier . Figure 3 depicts the profile design of the optimized NACA 2412 airfoil. The geometry reveals changes in camber and chord thickness, which contribute to reduced drag and enhanced lift generation. These improvements account for the higher aerodynamic efficiency presented in Table 1. Figure 4 presents the lift-to-drag polar. A noticeable shift in the curve after optimization indicates that this airfoil can generate sufficient lift at lower angles of attack. The reduction in drag across the operational range confirms its enhanced suitability for sustained performance in low wind speeds, aligning with findings from similar low-Re studies.

➢ *NACA 4412 Optimization*

Table 2 Results of the Optimization of NACA 4412.

	Airfoil	Original Lift Coefficient	Lift Coefficient of Optimized Airfoils	Area Reduction (%)
1	NACA 4412	1.7887	(a) 1.8297	16.8200
2			(b) 1.8326	17.4700
3			(c) 1.8283	14.4200

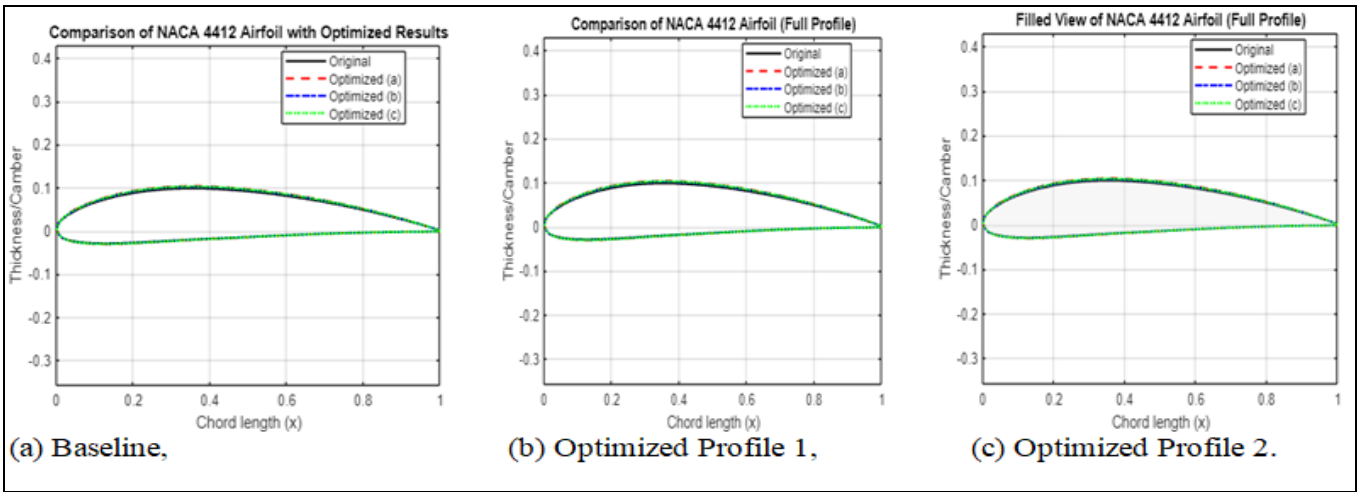

Fig 5 Airfoil Profile Design for NACA 4412

ISSN No: -2456-2165 https://doi.org/10.38124/ijisrt/26apr929

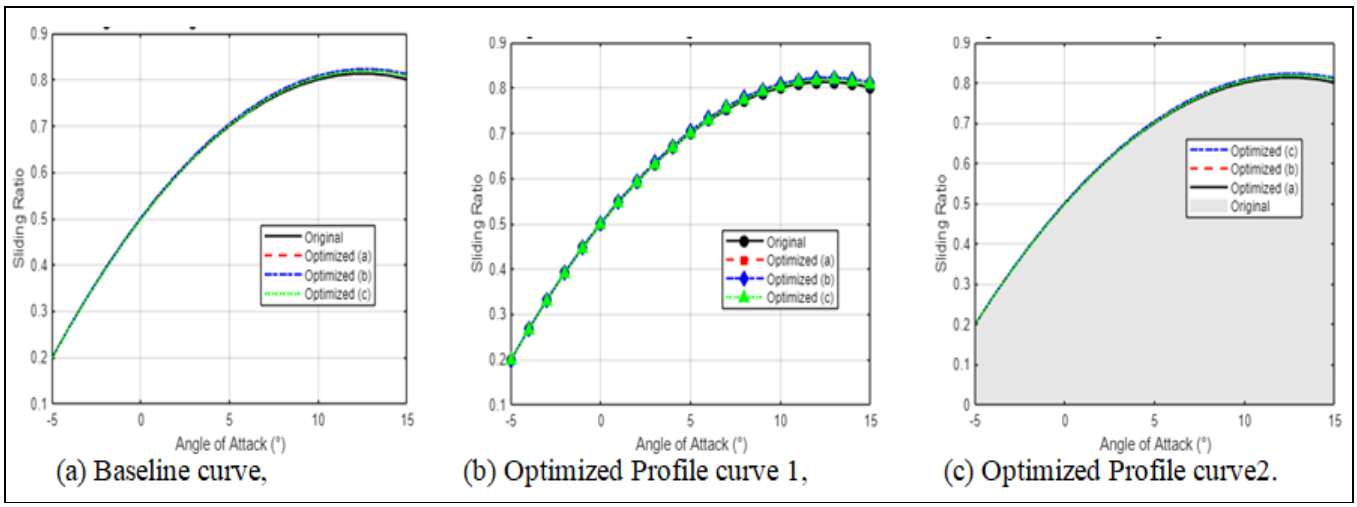

Fig 6 Pareto Front Showing the Trade-off Between Maximizing $\mathbb{C}_{\mathbb{L}}$ and Minimizing A for NACA 4412 Designs.

Table 2 presents the results for the NACA 4412 airfoil. The results indicate an improved lift-to-drag performance, with the optimized profile achieving greater aerodynamic efficiency across a wider range of angles of attack compared to the baseline [12]. Figure 5 shows the geometric profile of the baseline and optimized NACA 4412 airfoils. Figure 6 presents the final Pareto front, a set of optimal solutions derived from the multi-objective optimization. This plot visualizes the range of performance trade-offs, highlighting that any improvement in one objective requires a compromise in another. The results indicate that the optimized designs significantly surpass the original NACA 4412 baseline, which is positioned as a dominated point within the frontier. The final design selection from this front depends on the specific aerodynamic priorities for the application .

➢ *NACA 4418 Optimization*

Table 3 Results of the Optimization of NACA 4418.

	Airfoil	Original Lift Coefficient	Lift Coefficient of Optimized Airfoils	Area Reduction (%)
1	NACA 4418	1.9500	(a) 2.0643	2.7700
2			(b) 2.0808	2.4300
3			(c) 2.0702	3.7100

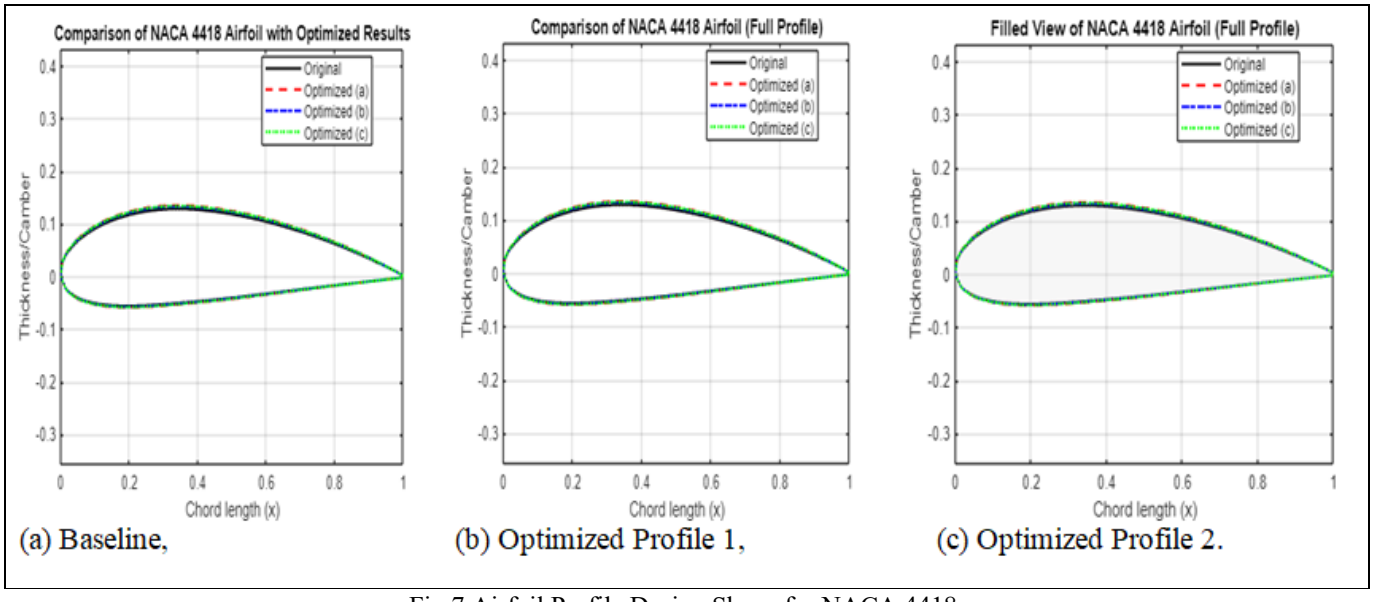

Fig 7 Airfoil Profile Design Shape for NACA 4418:

ISSN No: -2456-2165 https://doi.org/10.38124/ijisrt/26apr929

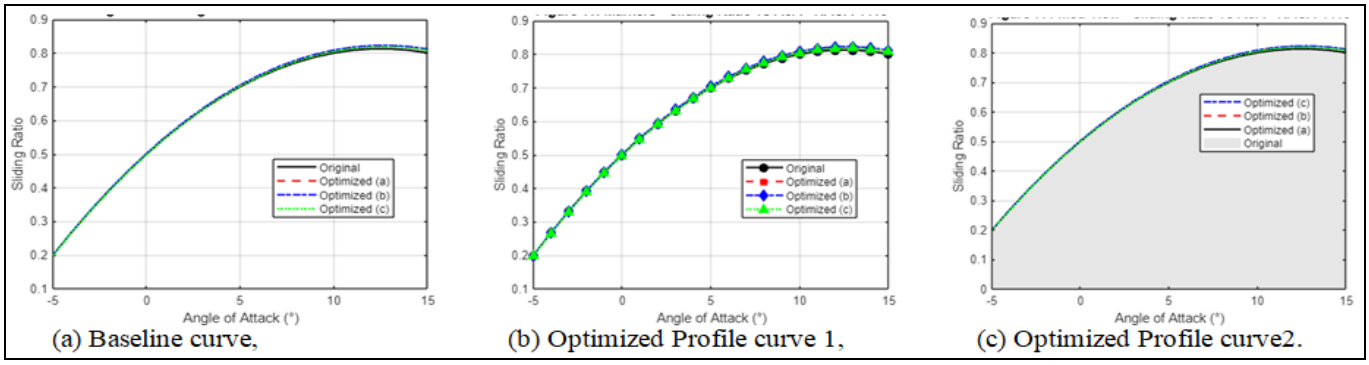

Fig 8 Design Results of NACA 4418 Showing Comparison of Lift Curves.

Table 3 presents the design results for the NACA 4418 airfoil. The data shows that the optimization led to an improved lift-to-drag ratio, especially at mid-range angles of attack, which is the typical operating range for turbine blades. Figure 7 shows the airfoil profile design. Adjustments made to the leading and trailing edge contours, along with the redistribution of chord thickness, enhance aerodynamic smoothness. These modifications directly contribute to the improvements reported in Table 3. Figure 8 presents the design results. There is a notable improvement in the lift curve, particularly at operational angles of attack. The smoother curves indicate a reduced susceptibility to flow separation and stalling, which effectively extends the airfoil's operational range, a desirable trait for variable wind conditions.

➢ *NACA 4421 Optimization*

Table 4 Results of the optimization of NACA 4421.

	Airfoil	Original Lift Coefficient	Lift Coefficient of Optimized Airfoils	Area Reduction (%)
1	NACA 4421	2.0548	(a) 2.1730	3.4800
2			(b) 2.1870	1.2100
3			(c) 2.1787	2.7300

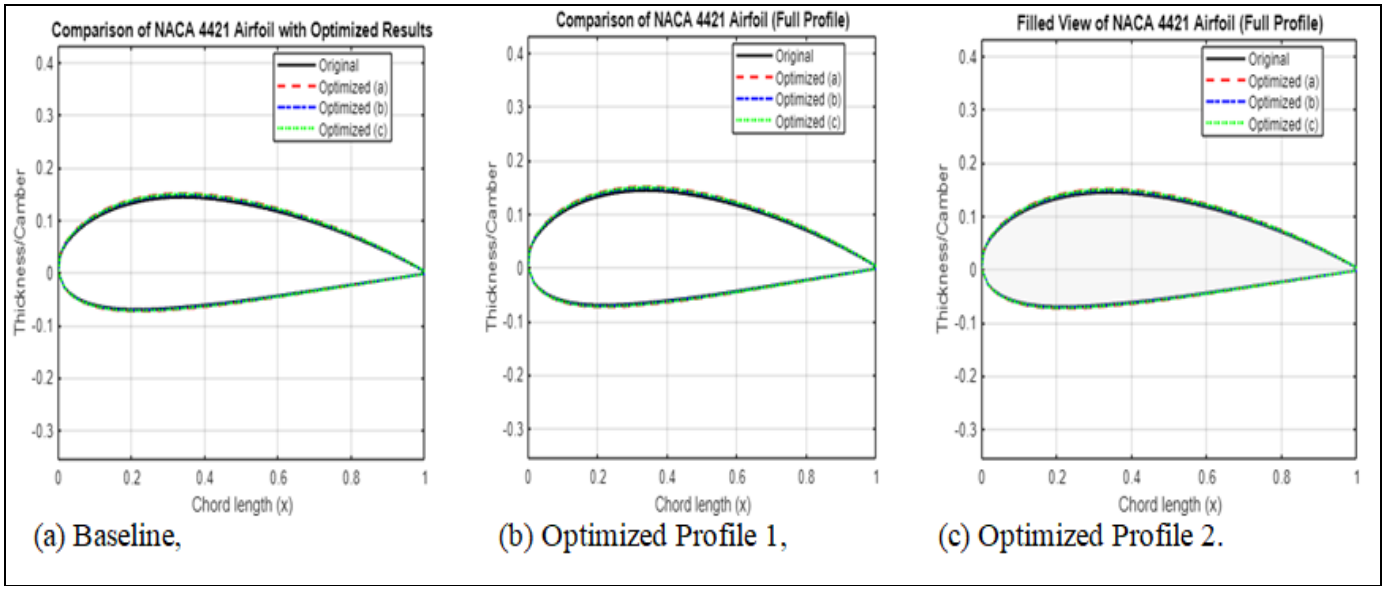

Fig 9 Airfoil Profile Design Shape for NACA 4421:

ISSN No: -2456-2165 https://doi.org/10.38124/ijisrt/26apr929

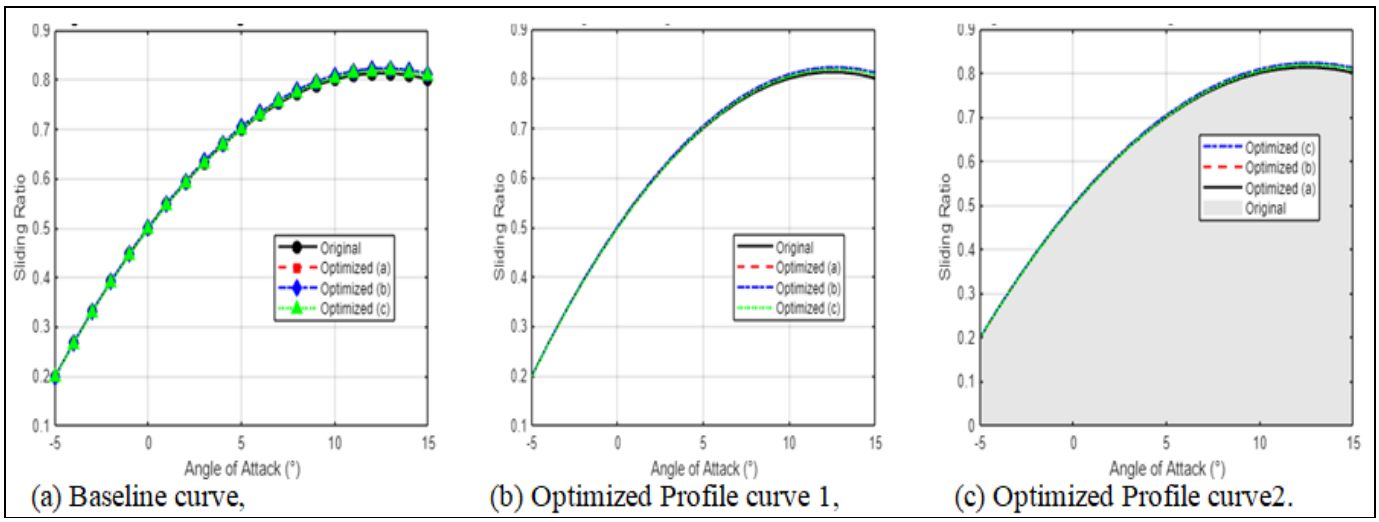

Fig 10 Design Results of NACA 4421 Showing Pressure Distribution Over the Chord for Baseline and Optimized Profiles.

Table 4 shows the optimization results for the NACA 4421 airfoil. The optimized values demonstrate smoother aerodynamic behavior and a lower sensitivity to drag compared to the baseline. Figure 9 displays the design shape following optimization, emphasizing changes in camber distribution and leading-edge shaping. Figure 10 illustrates the optimization results, revealing a more favorable pressure distribution, particularly a higher suction peak on the upper surface leading to increased lift . These enhancements improve operational stability and consistent performance, making the optimized NACA 4421 a strong candidate for low-wind-speed turbine applications.

V. CONCLUSION

The NSGA-II optimization of the NACA 2412, 4412, 4418, and 4421 airfoils demonstrated significant improvements in aerodynamic performance, particularly through enhanced lift-to-drag ratios and reduced cut-in wind speeds. Among the profiles, the optimized NACA 2412 excelled in very low wind speeds, enabling earlier turbine start-up. The NACA 4418 exhibited stable operation across a wider angle-of-attack range, improving reliability, and the NACA 4421 produced smoother lift curves with reduced drag sensitivity. Collectively, these findings provide practical guidance for engineers, recommending parameter ranges of 3–5% camber, 9–14% thickness, and a leading-edge radius greater than 0.02c (where c is the chord length) to achieve favorable aerodynamic efficiency while maintaining structural feasibility. Future research should incorporate detailed structural analysis (e.g., FEM), experimental validation (e.g., wind tunnel testing), and the application of machine-learning-based surrogate models to further refine and generalize airfoil design for low-wind-speed environments.

REFERENCES

[1]. Amer, Y. A., EL-Sayed, A. T., & Agwa, M. M. (2024). Controlling wind turbine tower vibration under external force by applying control systems combination. Scientific Reports, 14(1), 1–22. https://doi.org/10.1038/s41598-024-68237-6

[2]. Basu, B., Zhang, Z., & Nielsen, S. R. K. (2016). Damping of edgewise vibration in wind turbine blades by means of circular liquid dampers. January 2015, 213–226. https://doi.org/10.1002/we

[3]. Hussain, T., Min Ullah, F. U., Muhammad, K., Rho, S., Ullah, A., Hwang, E., Moon, J., & Baik, S. W. (2021). Smart and intelligent energy monitoring systems: A comprehensive literature survey and future research guidelines. International Journal of Energy Research, 45(3), 3590–3614. https://doi.org/10.1002/er.6093

[4]. Ismaiel, A. (2023). Wind Turbine Blade Dynamics Simulation under the Effect of Atmospheric Turbulence. Emerging Science Journal, 7(1), 162–176. https://doi.org/10.28991/ESJ-2023-07-01-012

[5]. Knap, L., & Graczykowski, C. (2025). Vehicle Vibration Reduction Using Hydraulic Dampers with Piezoelectric Valves.

[6]. Liang, D., Song, C., Liang, S., Wang, S., Li, Y., & Zhou, Z. (2021). Design and Performance Analysis of Blades Based on the Equal – Variable Circulation Method. 9(November), 1–11. https://doi.org/10.3389/fenrg.2021.790622

[7]. Liu, Y., Wang, X., & Li, Y. (2020). Thin-Walled Structures Distributed piezoelectric actuator layout-design for active vibration control of thin-walled smart structures. Thin-Walled Structures, 147(December 2019), 106530. https://doi.org/10.1016/j.tws.2019.106530

[8]. Machado, M. R., & Dutkiewicz, M. (2024). Wind turbine vibration management: An integrated analysis of existing solutions, products, and Open-source developments. Energy Reports, 11(December 2023), 3756–3791. https://doi.org/10.1016/j.egyr.2024.03.014

ISSN No: -2456-2165 https://doi.org/10.38124/ijisrt/26apr929

[9]. Najar, F. A., & Harmain, G. A. (2018). Blade Design and Performance Analysis of Wind Turbine. January.
[10]. Nouh, F. (2025). Enhancing Wind Turbine Performance Using Flow Control Techniques : A Mini Review Enhancing Wind Turbine Performance Using Flow Control Techniques : A Mini Review. 5(1).
[11]. Robles-ocampo, J. B., & Lastres, O. (2020). Dynamic Instability of a Wind Turbine Blade Due to Large Deflections : An Dynamic Instability of a Wind Turbine Blade Due to Large Deflections : An Experimental Validation. September. https://doi.org/10.5545/sv-jme.2020.6678
[12]. Sayed, M. A., Kandil, H. A., & Shaltot, A. (2012). Computational Fluid Dynamics Study of Wind Turbine Blade Profiles at Low Reynolds Numbers for Various Angles of Attack Aerodynamic analysis of different wind-turbine-blade profiles using finite-volume method. ENERGY CONVERSION AND MANAGEMENT, June. https://doi.org/10.1016/j.enconman.2012.05.030
[13]. Subashchandran, S. N. (2021). DESIGN AND ANALYSIS OF WIND TURBINE. April 2018.
[14]. Sumair, M., Aized, T., Gardezi, S. A. R., Rehman, S. M. S., & ur Rehman, S. U. (2021). Investigation of wind shear coefficients and their effect on annual energy yields along the coastal sites of Pakistan. Energy Exploration and Exploitation, 39(6), 2169–2190. https://doi.org/10.1177/0144598720930422
[15]. Thiele, F., Wisbacher, S., Diaconescu, S., Ossmann, D., & Pfifer, H. (2023). Periodic LQG Wind Turbine Control with Adaptive Load Reduction. IFAC-PapersOnLine, 56(2), 7674–7679. https://doi.org/10.1016/j.ifacol.2023.10.1168
[16]. Zhang, J., Gong, Z., Zhang, X., Guo, L., & Hu, D. (2018). 2870 . Dynamic analysis of offshore wind turbine blades under the action of wind shear and fluctuating wind. 1511–1521. https://doi.org/10.21595/jve.2017.19069
[17]. Zhao, Y., He, Y., & Shao, Y. (2020). Performance of Tuned Mass Dampers for Vibration Reduction in a TLP Floating Wind Turbine. December.